KEK 83-30
March 1984
P

AN EXAFS SPECTROMETER ON BEAM LINE 10B AT THE PHOTON FACTORY

Hiroyuki Oyanagi
Electrotechnical Laboratory, Sakura-mura, Niihari-gun,
Ibaraki 305, Japan

Tadashi Matsushita
Photon Factory, National Laboratory for High Energy Physics,
Oho-machi, Tsukuba-gun, Ibaraki 305, Japan

Masahisa Ito
The Institute of Physical and Chemical Research,
Wako, Saitama 351, Japan

and Haruo Kuroda
Department of Chemistry and Research Center for Spectrochemistry,
University of Tokyo, Hongo, Bunkyo-ku, Tokyo 113, Japan

NATIONAL LABORATORY FOR
HIGH ENERGY PHYSICS

KEK Reports are available from:

Technical Information Office
National Laboratory for High Energy Physics
Oho-machi, Tsukuba-gun
Ibaraki-ken, 305
JAPAN

Phone: 0298-64-1171
Telex: 3652-534 (Domestic)
(0)3652-534 (International)
Cable: KEKOHO

AN EXAFS SPECTROMETER ON BEAM LINE 10B AT THE PHOTON FACTORY

Hiroyuki Oyanagi
Electrotechnical Laboratory, Sakura-mura, Niihari-gun,
Ibaraki 305, Japan

Tadashi Matsushita
Photon Factory, National Laboratory for High Energy Physics,
Oho-machi, Tsukuba-gun, Ibaraki 305, Japan

Masahisa Ito
The Institute of Physical and Chemical Research,
Wako, Saitama 351, Japan

and Haruo Kuroda
Department of Chemistry and Research Center for Spectrochemistry,
University of Tokyo, Hongo, Bunkyo-ku, Tokyo 113, Japan

Abstract

An EXAFS spectrometer installed on the beam line 10B at the Photon Factory is designed to cover the photon energy between 4 and 30 keV. Utilizing either a channel-cut or two flat silicon crystals as a monochromator, a beam intensity between 10^8 and 10^9 photons/sec is obtained at 9 keV with a resolution of 1 eV. The performance of the spectrometer, such as a signal-to-noise ratio or an energy resolution is demonstrated with examples of K edge absorption spectra of bromine, germanium, galium arsenide, and zinc selenide.

KEYWORDS: synchrotron radiation, EXFAS, XANES, X-ray absorption spectrometer

1. Introduction

X-ray absorption spectroscopy (XAS) has successfully been applied to a numerous number of materials to study electronic and structural environments around an absorbing atom for the past decade. Analysis of the extended X-ray absorption fine structure (EXAFS) provides information on bond distance, coordination number, Debye-Waller factor, and in some cases, species of scattering atom surrounding an excited atom.[1),2)] On the other hand, the X-ray absorption near edge structure (XANES) contains the useful information on the density of states of conduction band near the Fermi level or site symmetry of scatterer atoms.[3)]

Recent extensive XAS studies on physical, chemical, and biological systems are partly due to the availability of synchrotron radiation from multi-GeV electron storage ring.[4)] The intense continuum from electron storage rings are particularly suitable as a light source for XAS experiments, since the modulation of absorption coefficient in the EXAFS region (>50 eV above edge) extends over a wide energy rang (500 - 1000 eV). It is required to accumulate more than 10^6 photons per data point of an EXAFS spectrum in order to obtain photon statistics better than 0.1%. Using a conventional sealed X-ray tube and a flat crystal monochromator, a typical photon flux is 10^3 photons/sec, so that it took two to three weeks to obtain data of a good quality.[5),6)] Even if a bent-crystal monochromator[7),8)] and a rotating anode X-ray generator[7)] are used in combination, the photon flux improves by three orders of magnitude with a medium energy resolution (10 eV at 9 keV), resulting in a data aquisition time of several to a few tens hours. Using a synchrotron radiation emitted from a multi- GeV electron storage ring the data collection time is reduced to a

few tens of minutes with much better resolution (for example, 1 eV at 9 keV) and statistics.

From June, 1982, synchrotron radiation from a 2.5 GeV electron storage ring at the Photon Factory became available. We report here the design and performance of the EXAFS spectrometer on Beam Line 10B at the Photon Factory. The spectrometer was commissioned in June 1982, and is now routinely used for EXAFS and XANES experiments in an absorption mode.

2. System configuration

A schematic diagram of the EXAFS spectrometer on BL 10B at the Photon Factory is shown in Fig. 1. A broad band synchrotron radiation is monochromatized by a double-crystal monochromator and passes through a sample placed between two ionization chambers. Two ionization chambers and a sample chamber or a cryostat are mounted on a lifting table which tracks the output beam height by computer control. The outputs from the ionization chambers are amplified and digitalized to calculate the absorbance of a sample by taking a log ratio of the two outputs. Absorption spectra are displayed on a CRT screen and the data are stored on a floppy disc for further data handling.

2.1 Light source and Beam Line

The power spectrum of the storage ring of the Photon Factory is shown in Fig. 2. The critical energy is 4.1 keV, above which the intensity decreases rather steeply. At present, a typical beam current is 100 mA with a life time of about 10 hours when the storage ring is operated at 2.5 GeV. The X-ray beam with a horizontal divergence of 2 mrad is extracted from the storage ring through a dual 0.2 mm thick beryllium

windows. The X-ray beam travels through a helium atmosphere to the entrance slit and the monochromator crystal which is placed 22 m from the source point of radiation. The actual intensity profile in the low energy region (< 6 keV) is modified by the transmission of beryllium windows and helium atmosphere in the beam transport system.

The beam size in the horizontal and vertical direction is limited by the entrance slit system. A 50 μm thick Kapton film is used as a window to separate the helium-filled section from the atmospheric section.

2.2 Monochromators

A double-crystal monochromator is designed to cover the photon energy between 4 and 30 keV with a high energy resolution and a rapid tunability. A channel-cut silicon (311) crystal or two plane parallel silicon (220) and (111) crystals are utilized. The energy of X-rays diffracted by an (hkl) lattice plane is given by

$$E_{hkl} = 12398.52/2d_{hkl} \sin\theta_B \text{ (eV)} \quad , \qquad (1)$$

where d_{hkl} is the d spacing in angstrom unit for an hkl reflection and θ_B the Bragg angle. The energy resolution of the instrument is given by

$$\Delta E/E = \sqrt{(\delta\theta_w)^2 + (\delta\theta_g)^2} \cot\theta_B \quad , \qquad (2)$$

where $\delta\theta_g$ is the angular divergence and $\delta\theta_g$ is the width of a crystal rocking curve, or the Darwin width. $\delta\theta_w$ for silicon (311) and (111) are 1×10^{-5} rad and 4×10^{-5} rad, respectively. $\delta\theta_g$ is 7×10^{-5} rad with a 1 mm entrance slit placed 22 m from the source point. The total energy

resolution of the instrument is estimated to be 1 eV at 9 keV when Si (311) reflection is used.

Figure 3 shows the geometry of a double crystal monochromator schematically. The output beam height H measured from the level of the incoming beam is expressed by

$$H = 2D \cos\theta_B \quad , \qquad (3)$$

where D is the spacing between two faces of a channel. The lifting table is controlled by a microcomputer to follow the output beam within an accuracy of 20 μm. The monochromator crystals are mounted on a goniometer which can be rotated with the minimum step of 0.1 arc sec by use of a microcomputer-controlled stepping motor. A fine adjustment of the first crystal can be made by a PZT (piezo-electric translator) when separate two crystals are used. This mechanism is also used as a means to detune the first crystal with respect to the second in order to eliminate the higher harmonics.

2.3 Detector

The detectors are two ionization chambers filled with pure nitrogen or a mixture of noble gas and nitrogen of atmospheric pressure. The copper electrodes of ionization chambers have a spacing of 10 mm and width of 60 mm. Two types of ionization chambers with the lengths of 140 mm and 280 mm are made. Kapton films with thickness of 50 μm are used as windows. The front chamber, (I_0-chamber), is required to absorb 10 - 20% of the photon flux while the second chamber, (I-chamber) should absorb the most of transmitted X-rays. Figure 4 shows the calculated absorption

$\ln(I_0/I)$ of the two types of ionization chambers for various kinds of mixture gas. a, c, and e are the absorption curves for 140 mm long chambers filled with pure nitrogen, a 25% - 75% argon-nitrogen mixture, and 50% - 50% argon-nitrogen mixture, respectively. b, d, and f are those for a 280 mm long chambers filled with pure nitrogen, a 25% - 75% argon-nitrogen mixture, and a 50% - 50% argon-nitrogen mixture, respectively. The downstream chamber is 280 mm long and absorbs 98% of the transmitted beam at 11 keV when it is filled with pure argon and operated at atmospheric pressure. However, in the higher photon energy region, say 25 keV, this chamber only absorbs 75% of the photon flux. In such a case, two 280 mm long ionization chambers are mounted in series and the sum of two outputs is measured in the high energy region (> 20 keV). The gas filled in the chambers is pressure-controlled and flows at approximately 15 cc/min.

2.4 Sample holder and data acquisition system

Samples can be held in a cryostat or a high temperature chamber, both of which are placed on a lifting table. The cryostat is equipped with a closed-cycle helium refrigerator, and the sample temperature can be controlled with an accuracy of 1 K over the range from 8.5 K to room temperature. Since two samples can be mounted on a copper holder fixed to the cold head of the cryostat, measurements of EXAFS spectra can be made conveniently in succession without braking the vacuum. The high temperature chamber can be filled with various kinds of gases.

The output currents of two ionization chambers are amplified by KEITHLEY 427 current-to-voltage amplifier and converted into frequencies proportional to the magnitude of output voltage to be digitally stored in

the dual gated scalers which count the outputs of two ionization chambers for a fixed time. The absorption spectrum is monitored on a CRT screen in real time and digital data are stored in a floppy disk for further data analysis. Digital data are also printed out with a line printer and absorption spectra are plotted by use of an x-y plotter.

3. Performance

3.1 Intensity and signal-to-noise ratio

The photon flux at Cu K-edge (9 keV) passing through a 1 $mm^{(V)}$ x 6 $mm^{(H)}$ aperture is $\sim 10^{8}$ photons/sec with a silicon (311) channel-cut monochromator when the storage ring is operated at 2.5 GeV and 60 mA. The energy resolution is approximately 1 eV. The photon flux increases by an order of magnitude if two flat silicon (111) crystals are used under the same condition. Ion currents of ionization chambers are of the order of 10^{-9} - 10^{-10} A, while the noise currents created in an amplifier is less than 10^{-13} A. Thus the total signal-to-noise ratio of absorption spectra is primarily determined by the photon statistics. However, care must be taken to minimize the electrostatical noise and leakage currents in ionization chambers.

A log ratio of two outputs of ionization chambers is expressed by the following equation when higher harmonics are neglected.

$$\ln(i_0/i) = \ln\{(1 - e^{-\mu_1 t_1}) / e^{-\mu_1 t_1})\} + \mu_s d \qquad (5)$$

where i_0 and i are ion currents of I_0 and I chambers. μ_1 is the absorption coefficient for I_0 chamber gas and t_1 the effective length of the ionization chamber. μ_s and d denote the absorption coefficient and

thickness of a sample. Here, the second chamber is assumed to completely absorb the transmitted X-rays. The first term in the right hand of Eq. (5) is due to the absorption by I_0 chamber and varies smoothly with photon energy. One can determine this term simply by taking a log ratio of i_0/i without a sample. The optimum absorption coefficient, or the best choice of I_0 chamber gas, is obtained by maximizing a signal-to-noise ratio of the EXAFS oscillations by use of Eq. (5).

K-edge absorption spectra for some simple compounds were measured in order to evaluate the performance of the spectrometer. Figure 5 shows Ge K-edge absorption spectrum for crystalline germanium taken at 80 K. A 25% - 75% argon-nitrogen gas mixture was used as the front chamber gas. The pre-edge region is approximated by a polynomial of the form: $\alpha E^{\beta} + \gamma$. The parameters α, β, and γ are determined by a least-squares fit to the pre-edge data. The oscillatory part $\chi(k)$ was obtained by subtracting the smooth background approximated by a cubic spline function and then by normalizing it with this background. Ge K-edge EXAFS thus obtained is plotted in Fig. 6 as a function of photoelectron wave number k. The absorption spectrum was measured in 30 minutes with an integration time of 1 second per point. The Fourier transform of $k\chi(k)$ over a k range from 3.6 A^{-1} to 19 A^{-1} is shown in Fig. 7. Peak positions of Fourier transform are displaced from the real positions in radial distance due to the phase shift. The relative peak positions and their magnitudes agree well with those of the previous work.[9)]

3.2 Energy resolution

Figure 8 shows the energy resolution versus photon energy calculated for various monochromator crystals using Eq. (2). With a channel-cut

silicon (311) monochromator, Br K-edge absorption spectrum of bromine was measured in order to experimentally evaluate the instrumental resolution. Figure 9 shows the near edge structure on Br K-edge for bromine at room temperature. The origin of the horizontal scale is taken as 13.452 keV. The full width at half maximum (FWHM) of the sharp peak, due to 1s to 4p transition, near threshold (13.46 keV) is 3.5 ± 0.1 eV. From the observed FWHM, the instrumental energy resolution at 13.46 keV is estimated to be 2.8 eV provided that the life time broadening is 2 eV.[10] This corresponds to an energy resolution of 1.1 eV at 9 keV. It should be noted that the normalized magnitude of this sharp peak to the absorption coefficient at the onset of continuum (13.47 keV) is higher (1.39) in the present work than in the previous work (0.94).[11] This difference seems to indicate a better energy resolution of our spectrometer.

Figure 10 shows the near edge structure on Ga and As K-edges for crystalline gallium arsenide at room temperature. The derivatives of the absorption spectra are indicated by dotted lines. In both spectra, the fine structures with periods of 1 - 2 eV are observed. However, a small bump 10 eV below the Ga (cation) edge is absent in the near edge structure on As (anion) edge in spite of the similar near neighbor environments. The similar trend is observed in the near edge spectra of zinc selenide on Zn (cation) and Se (anion) edges, as shown in Fig. 11. These results suggest that the instrumental resolution of 1 - 2 eV is essential for XANES studies on solids.

In order to obtain such a high resolution, the spectrometer must be capable of positioning a monochromator crystal with a minimum step equivalent to energy increments of less than 1 eV near threshold. For instance, at Br K-edge (13.47 keV), the bragg angles for silicon (111) and

(311) reflections are 8.44 and 16.32 degrees. At this energy, energy increment of 1 eV correspond to 0.0006 and 0.0016 degrees in step angle, for Si (111) and Si (311) reflections, respectively. The rotation of goniometer is done with a step angle of 0.1 arc sec (1/36,000 degree) per pulse.

3.3 Higher harmonics

If the higher harmonics are present in the output beam from monochromator and their contributions are not neglected, a log ratio of i_0/i should be expressed as follows:

$$\ln (i_0/i) = \ln \{ \frac{1 - e^{-\mu_1 t_1}}{e^{-\mu_1 t_1} + A\varepsilon(1 - e^{-\mu_2' t_2})\, e^{(\mu_s - \mu_s')d}} \} + \mu_s d \qquad (6)$$

$$A = N_0(\lambda')/N_0(\lambda)$$

where $N_0(\lambda)$ and $N_0(\lambda')$ are the photon fluxes at the fundamental wavelength λ and higher harmonic wavelength λ', μ_1' and μ_2' denote the absorption coefficients of the first and second ionization chamber gas, respectively, μ_s' is the total absorption coefficient of a sample with thickness d at λ', ε is the relative ionization efficiency which is defined as a ratio of number of ions created by the same number of photons at the two wavelengths. We assumed that $e^{-\mu_1 t_1} \sim 1$ at λ'. It is now clear that the first term in the right hand of Eq. (6) contains the absorption coefficient of a sample and therefore is not separated by measuring a blank sample.

The intensity of the higher harmonics can be reduced in several ways. For instance, with a silicon (311) crystal, the second order reflection is

forbidden, so that twice higher energy component is very weak for such a crystal. The intensity of the third order reflection is small because the steep fall-off of the synchrotron radiation spectrum at high energies. By choosing an appropriate gas for ionization chamber the effect of higher harmonics is minimized with a sacrifice of an intensity. If the second ionization chamber gas is chosen so that it transmits the most of higher order reflection, or $(1 - e^{-\mu_2' t_2}) \sim 0$, Eq. (6) reduces to Eq. (5). Another method is based on the fact that the higher order reflection has a narrower Darwin width than that of the fundamental. The intensity of higher harmonics is expected to decrease rapidly when a parallel setting between the two flat crystals is slightly detuned.[12] How this method works to remove higher harmonics is checked by measuring intensity of X-ray beam monochromatized by silicon (220) crystals through a very small pin-hole with a pure germanium solid state detector. The intensity ratio of the fundamental and second order reflection was 0.137 at 9 keV, when two crystals are aligned in parallel. The intensity ratio of second reflection to the fundamental peak dropped to 0.005 by slightly detuning one of the crystals from the parallel position. The intensity of the fundamental reflection decreased by 28% due to this detuning procedure.

4. Concluding remarks

The performance of the EXAFS spectrometer on Beam Line 10B was found to be satisfactory for EXAFS and XANES in a transmission mode. It is now routinely used by users from various universities, national laboratories and private industries. Since June, 1982, beam times of this spectrometer have been assigned to more than 50 proposals. These experimental results are partly reported in Photon Factory Activity Report, 1982/83.[13]

Acknowledgements

The authors are grateful to Prof. K. Kohra and Prof. S. Hosoya for their continual encouragement. They want to thank Dr. T. Fukamachi for his help in the development of a microcomputer system, and Dr. T. Ishikawa for preparing a silicon channel-cut crystal monochromator. They also thank Dr. M. Nomura for designing an experimental hutch, Dr. M. Okuno for rewriting measurement program, Messrs. K. Asakura and H. Ishii for their help in the experiment, and members of 'EXAFS' working group for their useful discussions.

References

1) E.A. Stern, Phys. Rev. B10 (1974) 3027; F.W. Lytle, D.E. Sayers, and E.A. Stern, ibid B11 (1975) 4825; E.A. Stern, D.E. Sayers, and F.W. Lytle, ibid B11 (1975) 4836.

2) P.A. Lee, P.H. Citrin, P. Eisenberger, and B.M. Kincaid, Rev. Mod. Physics, 53 (1981) 769; T.M. Hayes and J.B. Boyce, Solid State Phys., 37 (1982) 173.

3) A. Balzarotti, A. Bianconi, E. Burettini, M. Grandolfo, R. Habel, and M. Piacentini, Phys. Status Solid B63 (1974) 77; P.J. Durham, J.B. Pendry, and C.J. Hodges, Solid State Commun. 38 (1981) 159.

4) H. Winich and S. Doniach, eds., "Synchrotron Radiation Research", Plenum, New York, 1980.

5) H. Oyanagi, K. Tsuji, S. Hosoya, S. Minomura, and T. Fukamachi, J. Non-Cryst. Solids 35-36 (1980) 555.

6) "Laboratory EXAFS Facilities - 1980", American Institute of Physics Conference Proceedings No. 64, edited by E.A. Stern, American Institute of Physics, New York, 1981.

7) P. Georgopoulos and G.S. Knapp, J. Appl. Cryst. 14 (1981) 3; G.G. Cohen, D.A. Fischer, J. Colbert, and N.J. Shevchik, Rev. Sci. Instrum. 51 (1980) 273; S. Khalid, R. Emrich, R. Dujari, J. Shultz, and J.R. Katzer, ibid 53 (1982) 22; W. Thulke, R. Haensel, and P. Rabe, ibid 54 (1983) 277.

8) A. Williams, Rev. Sci. Instrum. 54 (1983) 193.

9) T.M. Hayes, J. Non-Cryst. Solids 31 (1978) 57; P.A. Lee and G. Beni, Phys. Rev. B15 (1977) 2862.

10) The instrumental resolution curve can be approximated by a Gaussian curve, while the natural spectral line shape is a Lorentzian. The measured width is therefore neither the sum of the instrumental width and the natural line width, nor the root mean square of these. However, a maximum possible value for the instrumental resolution was estimated to be 2.8 eV at 13.4 keV by assuming both of the instrumental curve and the spectral line shape to be Gaussians. The energy spread (2 eV) of 1s core hole state of bromine is used as the line width, since the spread of the 4p bound state is negligibly small. For a detailed discussion, see K. D. Sevier, Low Energy Electron Spectroscopy, Wiley Interscience, New York (1972), Chap. 6.

11) B.M. Kincaid and P. Eisenberger, Phys. Rev. Lett. 34 (1975) 1362.

12) V. Bonse, G. Materlik and W. Schröder, J. Appl. Cryst. 9 (1974) 223.

13) Photon Factory Activity Report 1982/83, National Laboratory for High Energy Physics (1984).

Figure captions

Fig. 1 Schematic diagram for an EXAFS apparatus at the unfocused beam line 10B of Photon Factory. The X-ray beam travels through a helium atmosphere to an entrance slit and a double crystal monochromator. Intensities of incident and transmitted X-rays are measured by two ionization chambers.

Fig. 2 Power spectrum of synchrotron radiation at Photon Factory. The energy of stored electrons is 2.5 GeV. The photon flux is given for a 1% band width.

Fig. 3 Geometrical arrangement of a double-crystal monochromator. Output beam is displaced by $2D \cos\theta_B$ in vertical position from the height of the incident X-ray beam.

Fig. 4 Absorption of ion chamber gas for various mixtures and lengths of chamber. a, c, and e are absorption $\ln(i_0/i)$ for pure nitrogen, a 25% - 75% argon nitrogen mixture, and a 50% - 50% argon-nitrogen, mixture using a 140 mm long ion chamber. b, d, and f are for a 280 mm long ion chamber filled with the same gas mixtures as above.

Fig. 5 Ge K-edge absorption spectrum of crystalline germanium at 80 K as a function of photon energy. The sharp threshold at 11.11 keV is the onset of K-shell absorption.

Fig. 6 The EXAFS oscillation $\chi(k)$ on the Ge K-edge for crystalline germanium at 80 K as a function of photoelectron wave number. The oscillatory parts were obtained by fitting the smooth background with a cubic spline.

Fig. 7 The magnitude of Fourier transform F(r) of the EXAFS on the Ge K-edge in crystalline germanium at 80 K. The data were transformed using $\chi(k)$ between 3.6 and 19 A^{-1}.

Fig. 8 Energy resolution of the spectrometer as a function of photon energy for silicor (111), (220), and (311) crystals.

Fig. 9 Absorption spectrum near Br K-edge for bromine at room temperature. An arrow indicates the FWHM of a sharp spike at 13.46 keV due to the 1s - 4p transition.

Fig. 10 Near edge structure on the Ga K- and As K-edges for galium arsenide at room temperature. Derivatives of absorption spectra are indicated in dotted line. The origin of a horizontal scale is taken at 10.367 keV and 11.867 keV for Ga K- and As K-edges.

Fig. 11 Near edge structure on the Zn K- and Se K-edges for zinc selenide at room temperature. The origin of a horizontal scale is taken at 9.659 keV and 12.658 keV for Zn K- and Se K-edges, respectively.

EXAFS SPECTROMETER

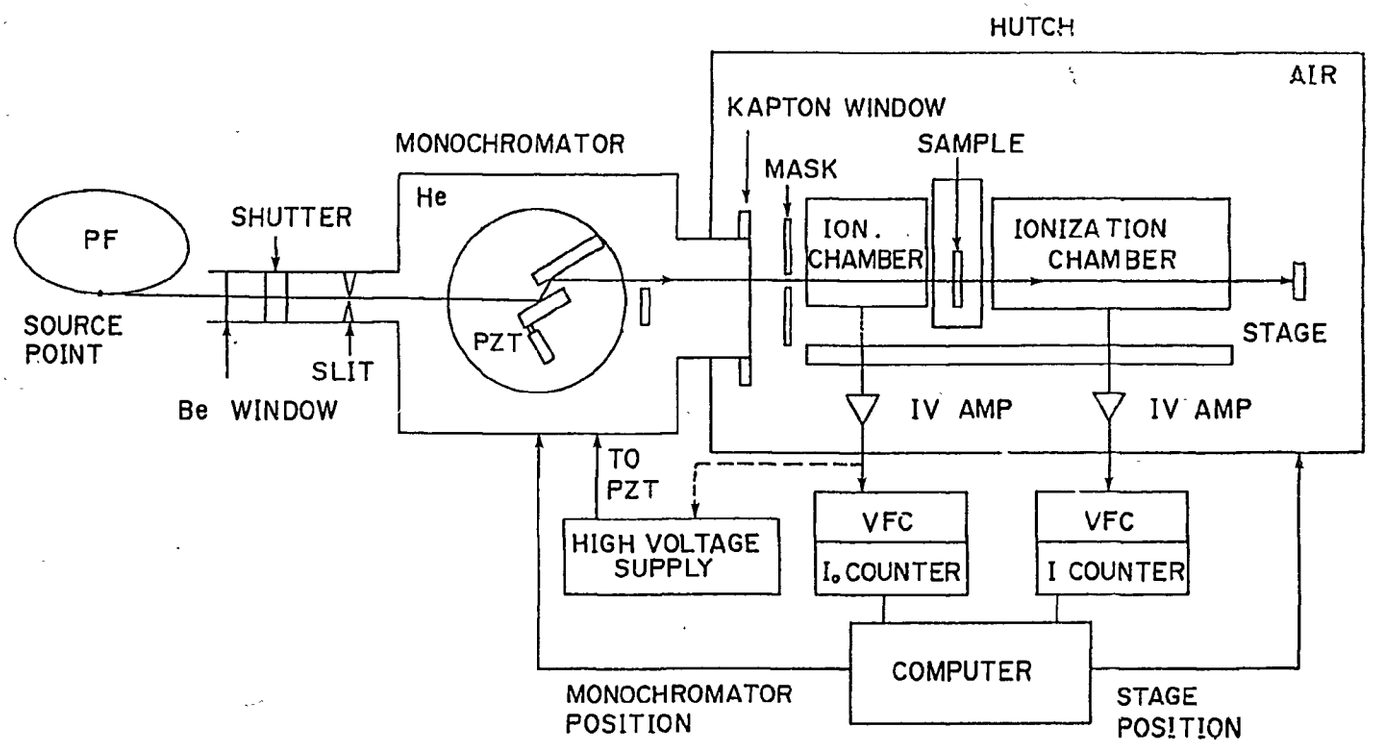

Fig.1

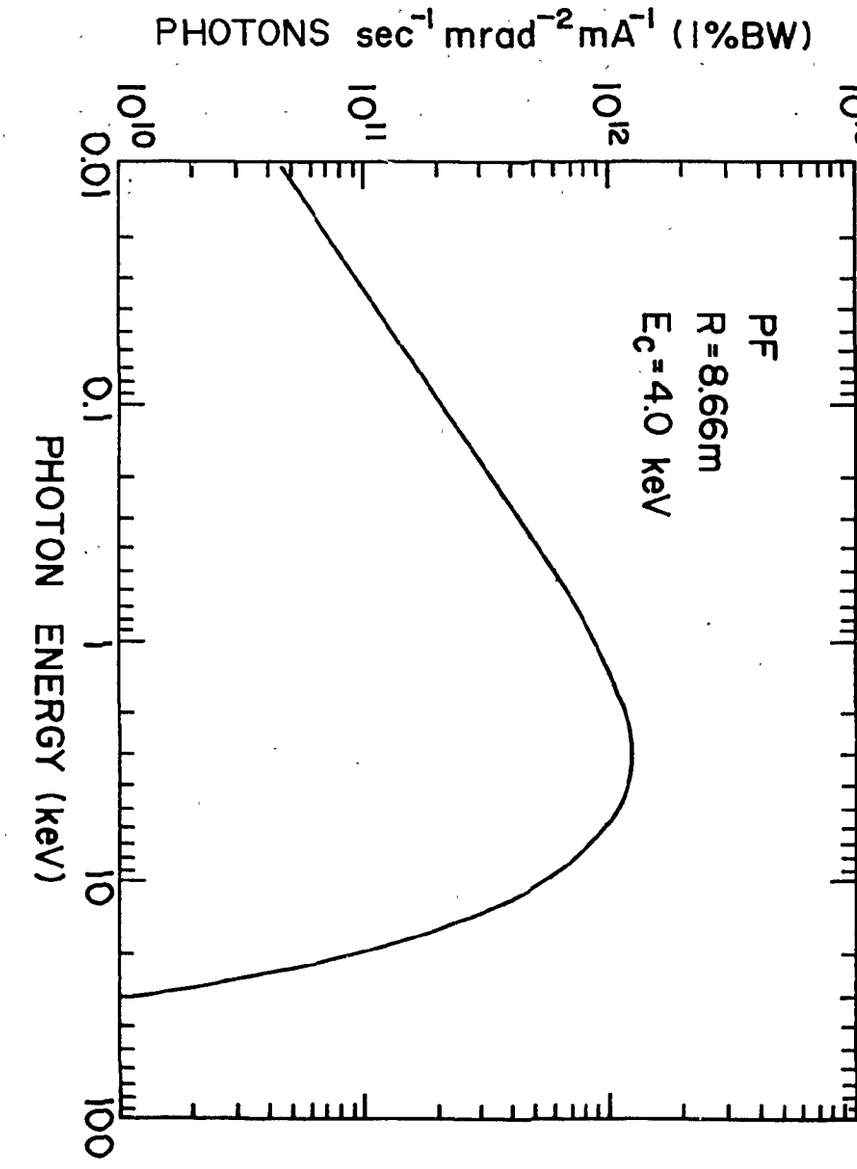
PHOTONS sec^{-1} mrad^{-2}mA^{-1} (1%BW)
10^{10}
10^{11}
10^{12}
10^{13}
0.01
0.1
1
10
100
PHOTON ENERGY (keV)
PF
R=8.66m
E_c=4.0 keV

Fig. 2

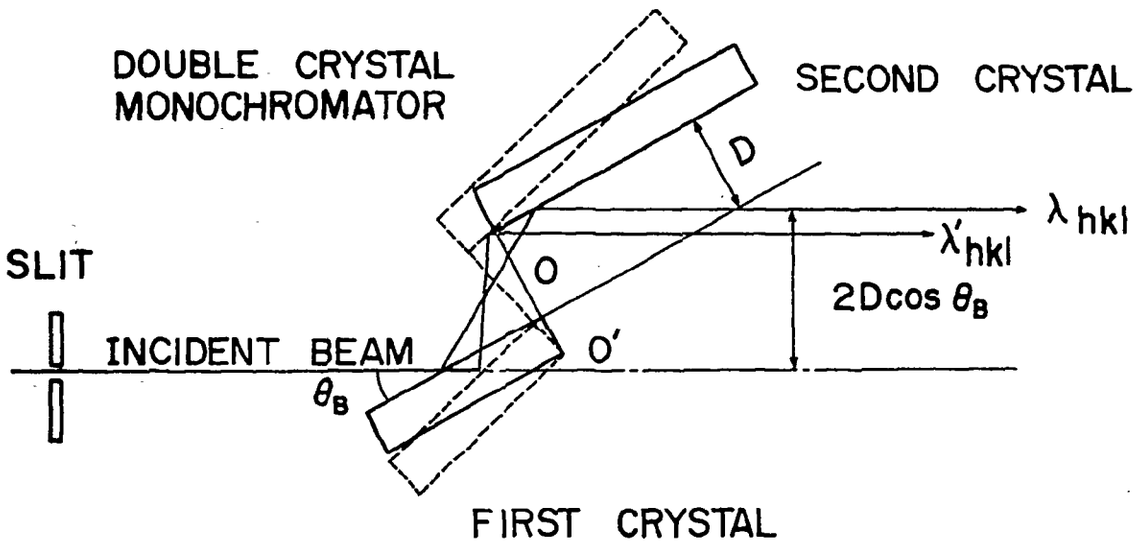
DOUBLE CRYSTAL
MONOCHROMATOR
SECOND CRYSTAL
D
λ hkl
λ'hkl
SLIT
O
2Dcos θB
INCIDENT BEAM
O'
θB
FIRST CRYSTAL

Fig. 3

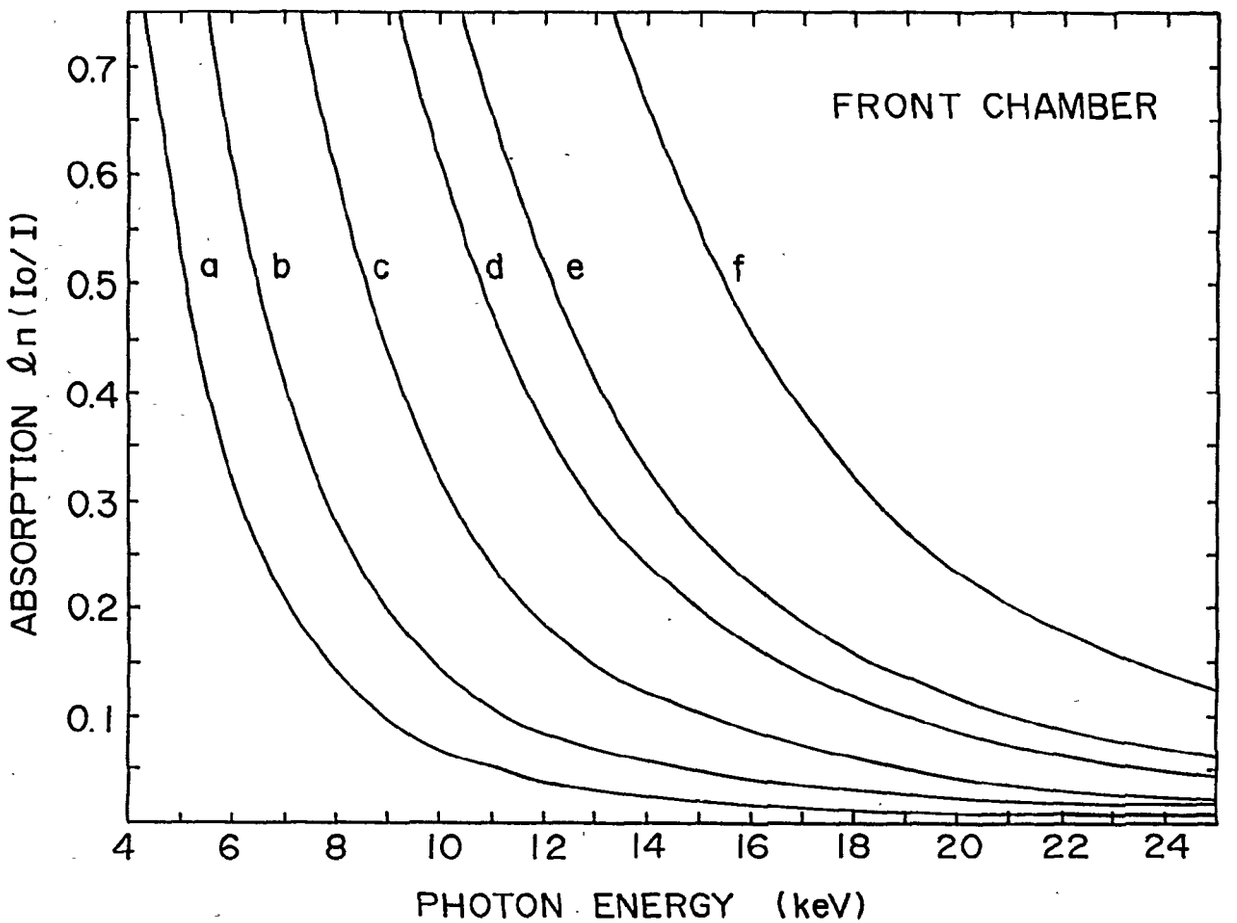
FRONT CHAMBER
ABSORPTION ℓn (Io/I)
0.7
0.6
0.5
0.4
0.3
0.2
0.1
a
b
c
d
e
f
4
6
8
10
12
14
16
18
20
22
24
PHOTON ENERGY (keV)

Fig. 4

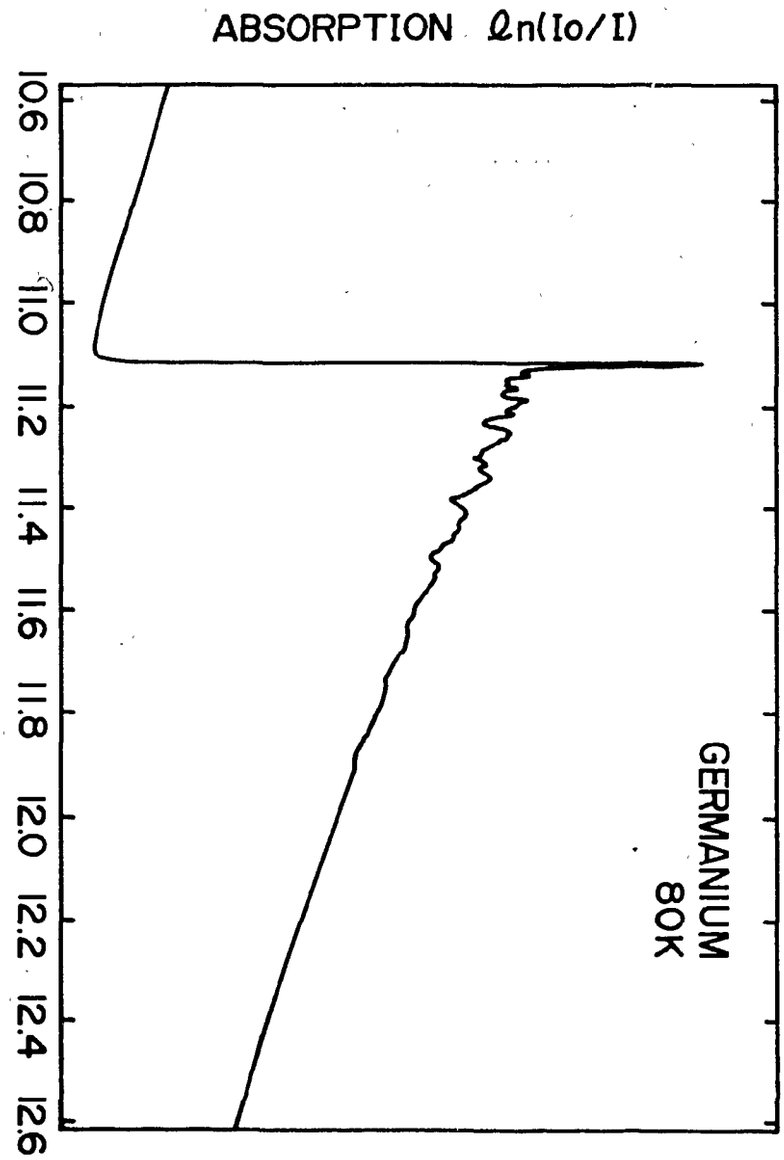
ABSORPTION ℓn(Io/I)
GERMANIUM
80K
10.6
10.8
11.0
11.2
11.4
11.6
11.8
12.0
12.2
12.4
12.6
PHOTON ENERGY (keV)

Fig. 5

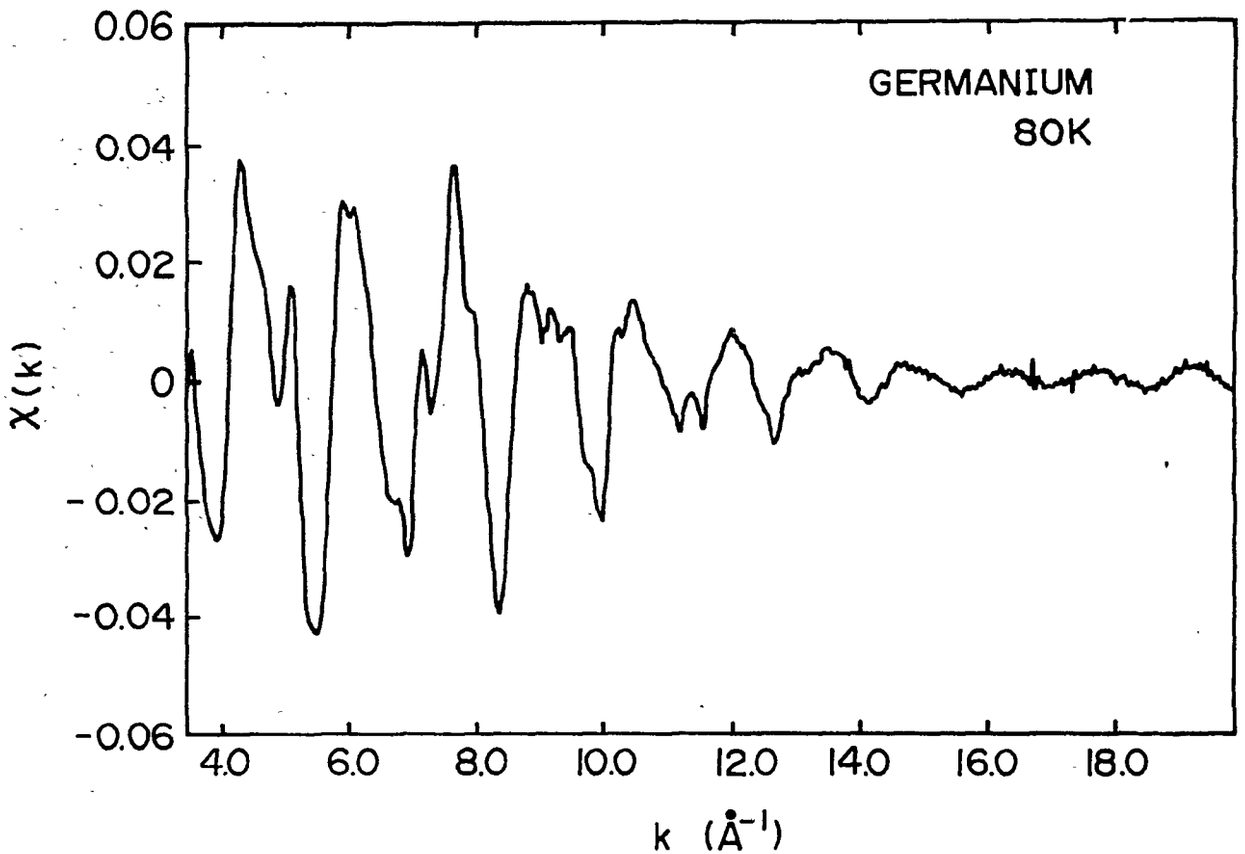
GERMANIUM
80K
0.06
0.04
0.02
0
-0.02
-0.04
-0.06
χ(k)
4.0
6.0
8.0
10.0
12.0
14.0
16.0
18.0
k (Å⁻¹)

Fig. 6

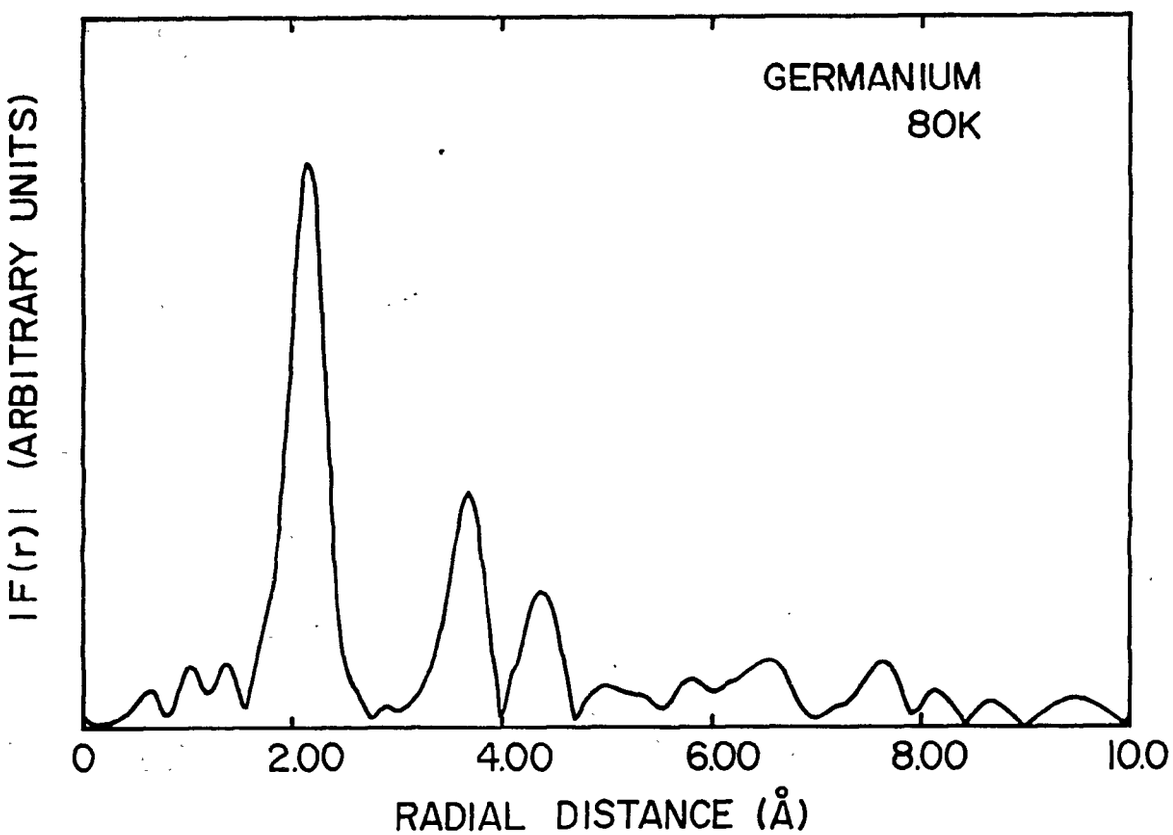
GERMANIUM
80K
|F(r)| (ARBITRARY UNITS)
0
2.00
4.00
6.00
8.00
10.0
RADIAL DISTANCE (Å)

Fig. 7

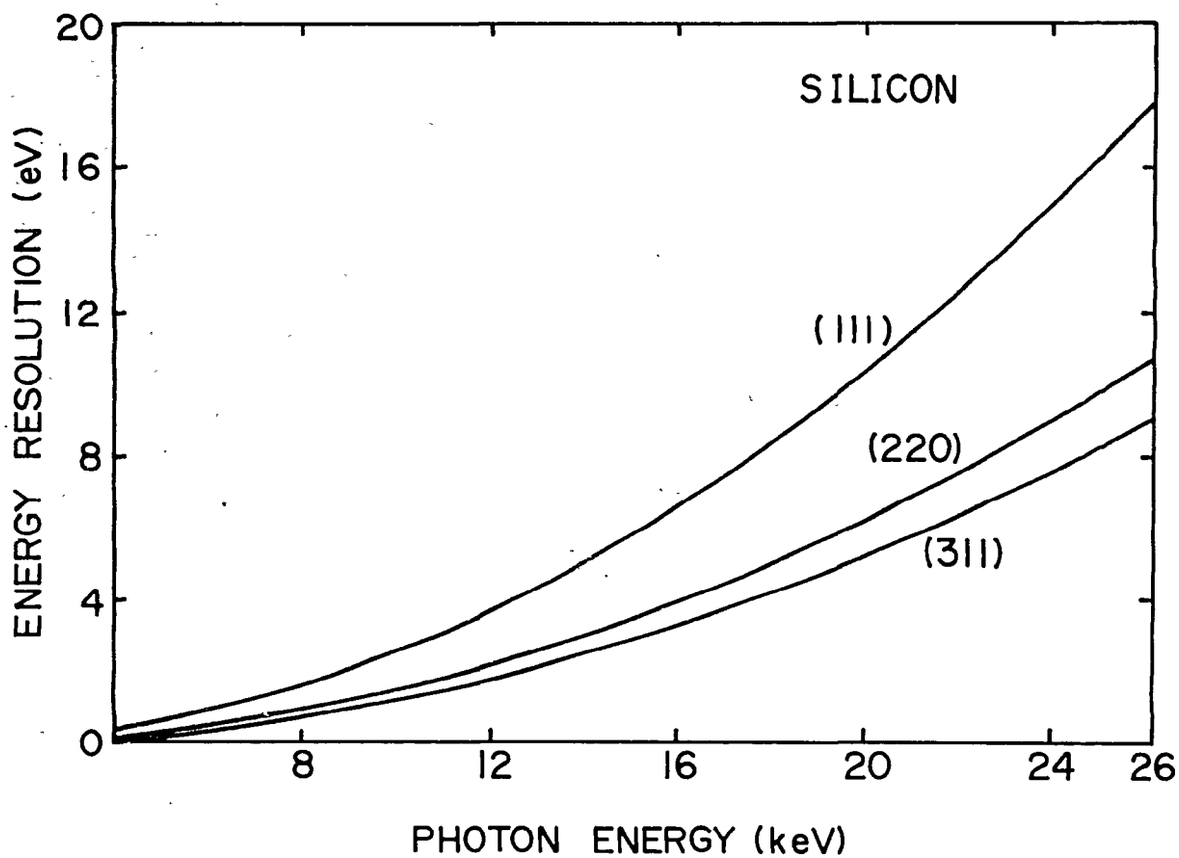
SILICON
(111)
(220)
(311)
ENERGY RESOLUTION (eV)
PHOTON ENERGY (keV)
0
4
8
12
16
20
8
12
16
20
24
26

Fig. 8

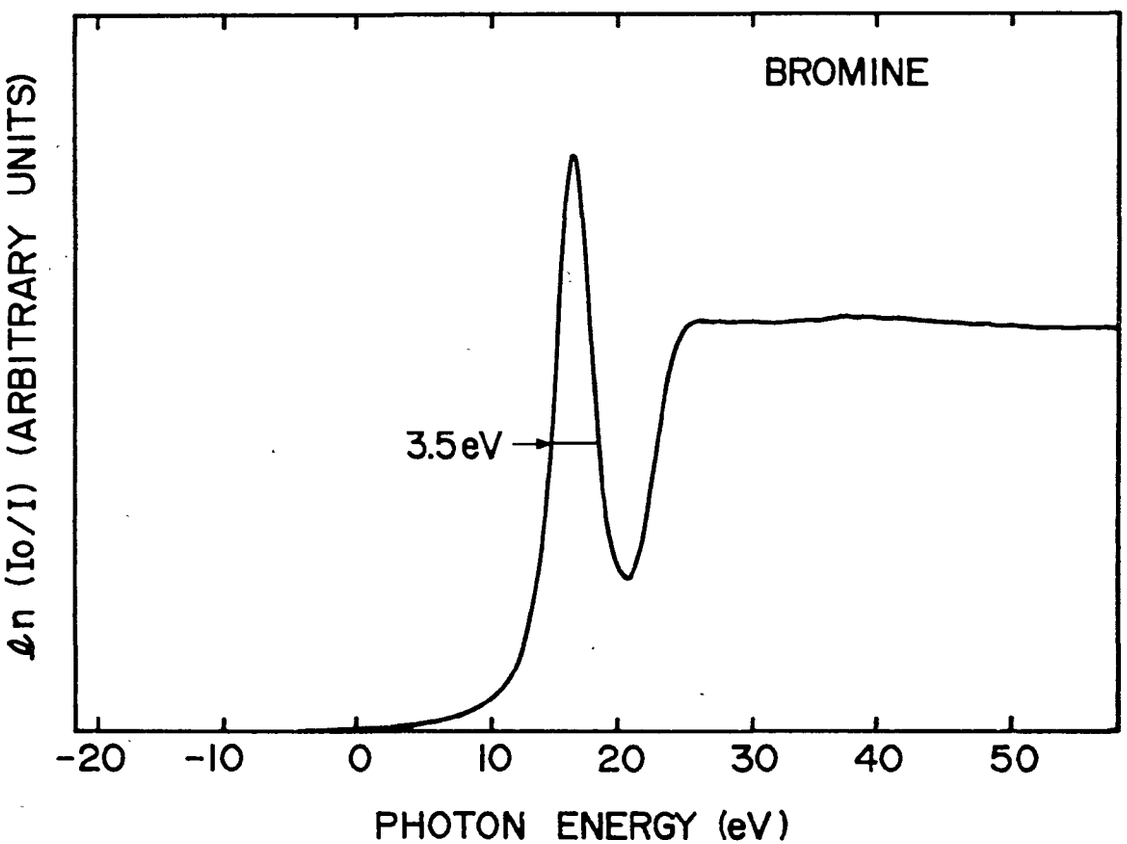
BROMINE
3.5eV
ln (Io/I) (ARBITRARY UNITS)
-20
-10
0
10
20
30
40
50
PHOTON ENERGY (eV)

Fig. 9

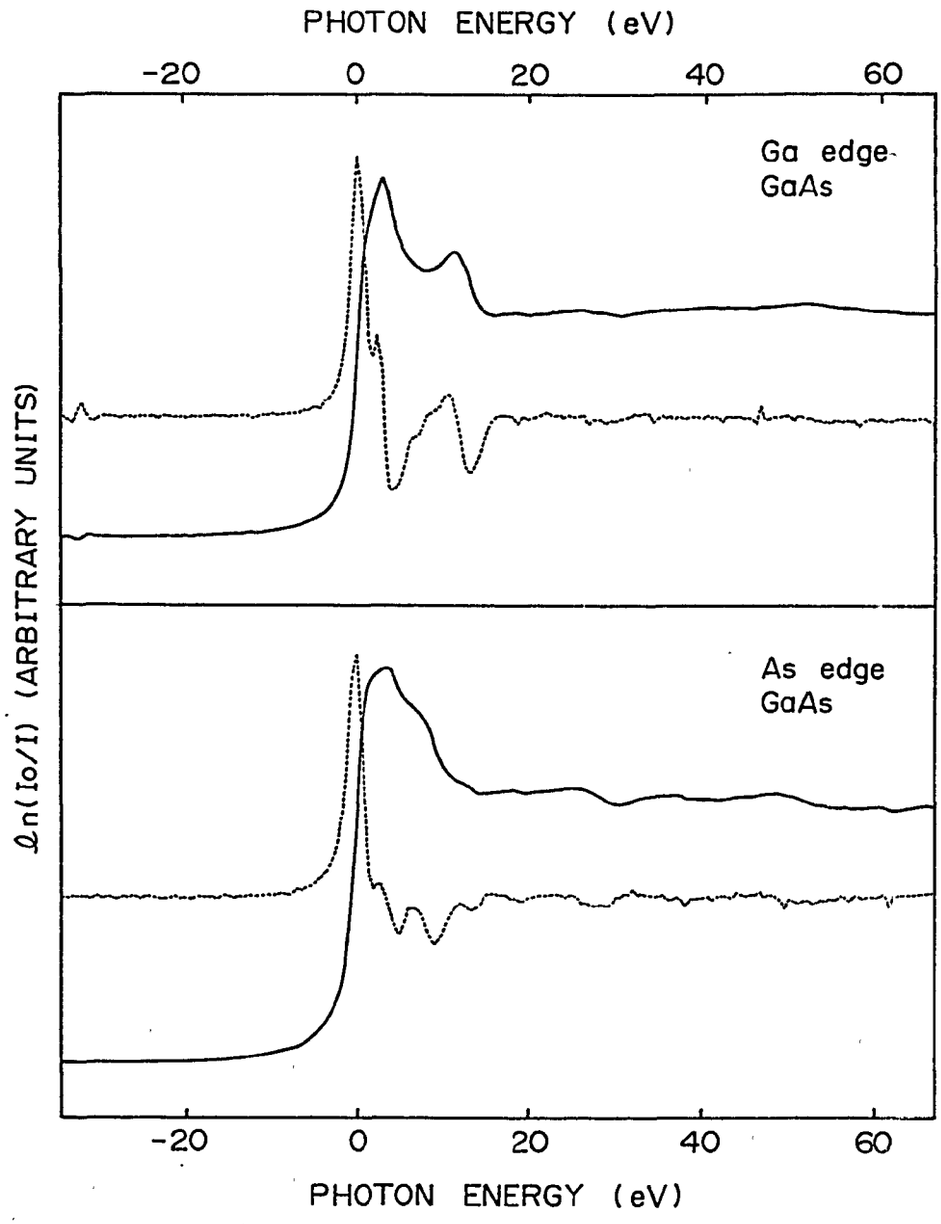
PHOTON ENERGY (eV)
-20
0
20
40
60
Ga edge
GaAs
As edge
GaAs
ℓn(Io/I) (ARBITRARY UNITS)
-20
0
20
40
60
PHOTON ENERGY (eV)

Fig. 10

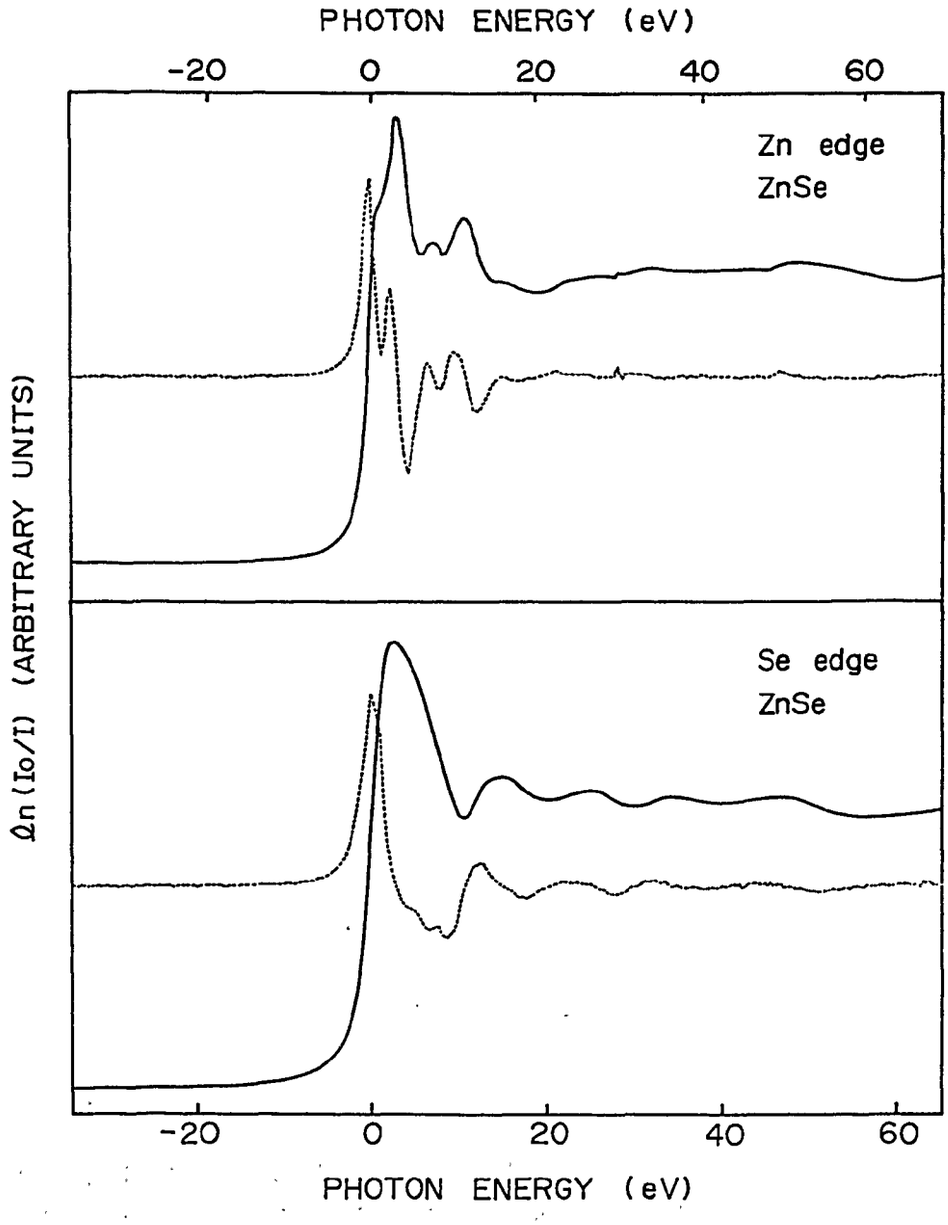
PHOTON ENERGY (eV)
-20
0
20
40
60
Zn edge
ZnSe
Se edge
ZnSe
ln (Io/I) (ARBITRARY UNITS)
-20
0
20
40
60
PHOTON ENERGY (eV)

Fig. 11